doi:10.1246/cl.2012.386
Published on the web March 24, 2012

CeO_2 Hollow Nanospheres as Anode Material for Lithium Ion Batteries

Manickam Sasidharan,[1] Nanda Gunawardhana,[2] Masaki Yoshio,*[2] and Kenichi Nakashima*[1]
[1]*Department of Chemistry, Faculty of Science and Engineering, Saga University, 1 Honjo-machi, Saga 840-8502*
[2]*Advanced Research Center, Saga University, 1341 Yoga-machi, Saga 840-0047*

(Received December 5, 2011; CL-111163; E-mail: nakashik@cc.saga-u.ac.jp, yoshio@cc.saga-u.ac.jp)

CeO_2 hollow nanospheres were synthesized using polymeric micelle poly(styrene-*block*-acrylic acid-*block*-ethylene oxide) with *core–shell–corona* architecture. The CeO_2 hollow nanospheres were investigated as anode materials for rechargeable lithium ion batteries for the first time. The nanostructured electrode shows desirable electrochemical properties such as high capacity, good capacity retention, and rate performance.

Lithium ion batteries (LIBs) due to their high energy density and low self-discharge rates compared to other types of batteries are dominant power sources for portable electronic devices. LIBs are also under active investigation worldwide as power sources in electric and hybrid automobiles.[1,2] The major challenges in constructing next-generation lithium-ion batteries include the need to increase their energy density, cycling life, and charge–discharge rate capability. The most commonly used graphite anode material has limited gravimetric capacity ($372\,mA\,h\,g^{-1}$), and extensive research has been focused to replace it with high-capacity transition-metal oxides. High irreversible capacity loss during the first several charge/discharge cycles and gradual breakdown of electrodes due to repeated cycling (capacity fading) are the main drawbacks. While the former is intrinsic for most anode materials, the latter is widely believed to result from large volume change. Specifically, large volume changes in the active particles leads to mechanical failure resulting in a steady capacity loss.

Generally, it is believed that when material sizes are reduced down to nanometer scale, they usually exhibit significantly enhanced functionalities in their properties.[3] For instance, hollow nanoparticles with spherical morphology are unique candidates with high mechanical strength, surface permeability, and high surface area. Hollow nanospheres with thin shell domain not only enhance the fast lithium insertion–deinsertion kinetics but also the hollow void could serve as an effective buffering medium.[4] Ceria nanoparticles (CeO_2) are widely used nanomaterial for applications such as catalysis, oxygen storage, and photoluminescence.[5–7] Due to its oxidizing capability, CeO_2 serves as a promising candidate in solid oxide fuel cells (SOFCs) which efficiently convert chemical energy to electrical energy.[8–12] However, lithium insertion on CeO_2 has been scarcely investigated to date. Recently, we have reported the fabrication of Nb_2O_5, CeO_2, and V_2O_5 hollow nanospheres using cationic polymeric micelles.[13] Herein, we report the fabrication of CeO_2 hollow nanospheres using anionic micelles unlike the previous report. ABC triblock copolymer poly(styrene-*block*-acrylic acid-*block*-ethylene oxide) (PS–PAA–PEO) with anionic COO^- was used as a template, and cerium(IV) sulfate was used as metal source. The hollow nanospheres were characterized by TEM, XRD, FTIR, and thermal analysis. The CeO_2 hollow nanospheres were further investigated as anode materials for rechargeable lithium ion batteries for the first time.

The preparation and characterization of PS-*block*-PAA-*block*-PEO are reported eleswhere.[14] The polymer was dissolved in distilled water at room temperature to obtain $0.5\,g\,L^{-1}$ micelle solutions, and the pH was adjusted to 9. The hydrodynamic diameter D_h (62 nm) and the ζ potential (−49 mV) of the micelles (pH 9) were obtained from dynamic light-scattering (DLS) and electrophoretic light-scattering (ELS) experiments, respectively. Nearly monodispersed spherical micelles with average diameter of ca. 40 ± 2 nm were estimated from the TEM image (not shown). The shell-forming block (PAA) with –COOH groups is highly soluble in water and thus plays the role of a reservoir and reaction site for $CeSO_4$ at pH 9. The detailed procedure of synthesis of hollow nanospheres is provided in the Supporting Information.[22] The Ce^{4+} cation effectively binds with anionic $-COO^-$ groups to form composite particles which upon calcinations provide the desired CeO_2 hollow nanospheres. FTIR spectrum of calcined CeO_2 hollow particles (Figure S1, Supporting Information[22]) shows vibrational bands at 520 and $1126\,cm^{-1}$ characteristics of Ce–O stretching vibrations. The sharp band at $1648\,cm^{-1}$ is assigned to bending vibration of H_2O molecules.[15] The absence of vibrational bands characteristics of C–H and C=C bonds from polymeric template confirms the effective removal of template by calcinations. The removal of polymeric templates further confirmed by TG/DTA analysis, and all the polymeric species were completely burned at 500 °C.

The phase purity and the crystal structure of the CeO_2 hollow nanospheres were examined by X-ray diffraction (XRD). Figure 1 shows the XRD pattern of CeO_2 hollow nanospheres. All the peaks of the hollow particles can be indexed to a face-centered cubic phase [space group: *Fm*3*m*] of ceria (JCPDS

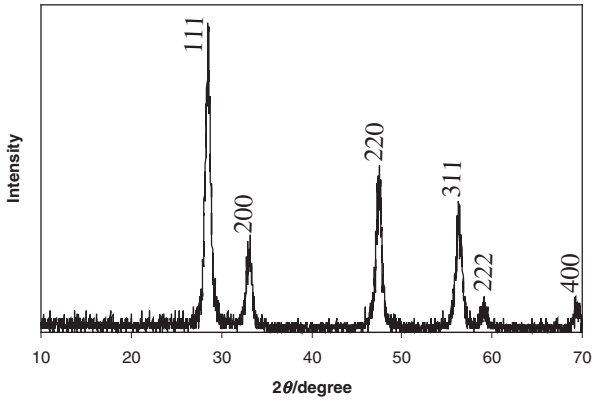

Figure 1. XRD pattern of CeO_2 hollow nanospheres.

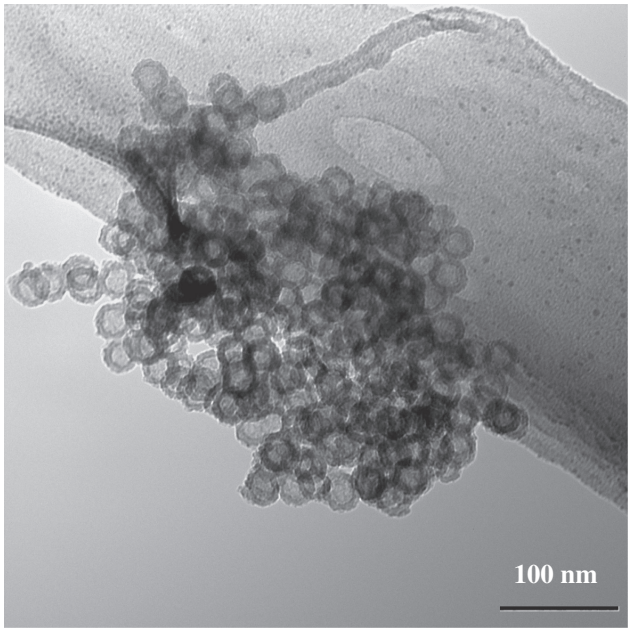

Figure 2. TEM image of CeO_2 hollow nanospheres.

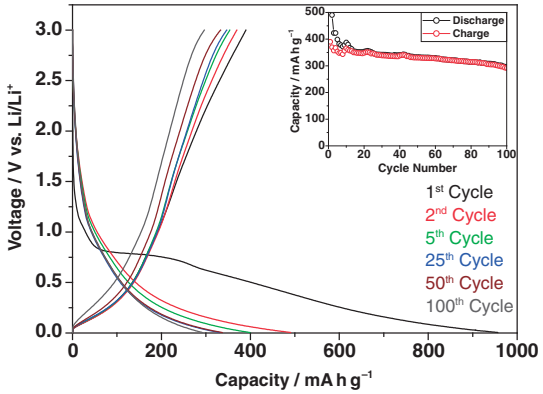

Figure 3. Capacity versus voltage profiles of CeO_2 hollow nanospheres at current density of 200 mA g^{-1}.

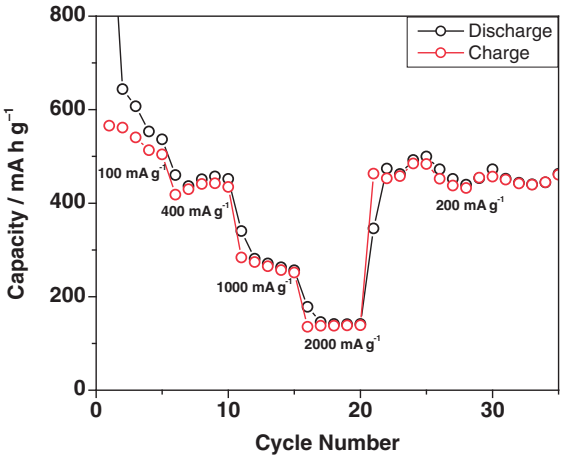

Figure 4. Rate performance of CeO_2 hollow nanospheres at different current densities.

No. 34-0394). It is noted that the peaks are obviously broadened, a typical feature of nanocrystalline CeO_2. The size and morphology of the CeO_2 particles were examined by transmission electron microscopy (TEM, JEOL, JEM 1210, 80 kV) observation. The TEM image (Figure 2) clearly shows the formation of hollow particles. The average diameter of hollow nanospheres was found to be 28 ± 2 nm, and the hollow void space 17 ± 1 nm. The shell thickness was estimated to be 5.5 ± 0.5 nm. Brunauer–Emmet–Teller (BET) surface area was 89 $m^2\,g^{-1}$ as estimated from nitrogen adsorption–desorption analyses. The above material was further investigated as anode material for lithium-ion rechargeable batteries.

The cyclic voltammograms of CeO_2 nanostructured electrode is shown in the Supporting Information (Figure S2).[22] In the cathodic polarization process of the first cycle, a reduction peak is appears at 0.33 V, while the anodic sweep showed a broad oxidation peak at about 0.3 V (vs. Li/Li^+). During the second cycle, the redox peaks appeared nearly at the same voltages albeit with low peak intensity. Therefore, the pair of peaks at 0.33 (cathodic) and 0.3 V (anodic) suggests the lithium insertion and deinsertion processes. Figure 3 shows the voltage versus capacity profiles of CeO_2 hollow nanosphere-based anode in the voltage window of 0.005–3.0 V (vs. Li/Li^+) at a current density of 200 mA g^{-1}. The highest discharge capacity of 956 mA h g^{-1} was observed in the first cycle. The high discharge capacity is ascribed to some irreversible lithium insertion into the crystal lattice which leads to irreversible capacity loss. The first discharge cycle exhibits a voltage plateau at about 0.8 V (vs. Li/Li^+) which continues up to a capacity of 290 mA h g^{-1} in accordance with the cathodic peak observed in the CV (Figure S2). Moreover, it is important to point out that the initial plateau and slope in the second and subsequent cycles were less obvious indicating an irreversible capacity loss in the first cycle similar to other dense as well as nanosized transition-metal oxides.[16–18] The discharge capacities in the 1st, 2nd, 5th, 25th, 50th, and 100th cycles are 956, 490, 398, 348, 332, and 296 mA h g^{-1}, respectively. The corresponding charge capacities are 390, 371, 354, 347, 331, and 291 for 1st, 2nd, 5th, 25th, 50th, and 100th cycles, respectively. Previously, the electrochemical performance of dense CeO_2 nanospheres was reported by Zhou et al.;[19] however, we cannot make any direct comparison because they used aluminum as a current collector which contributes to the total capacity through alloying–dealloying of aluminum with lithium. More importantly, CeO_2 hollow sphere-based anode delivers a capacity of 296 mA h g^{-1} after 100 cycles of repeated charge–discharges and maintains the electrode stability.

In Figure 3, the inset picture shows the discharge–charge capacities versus the cycle number in the voltage window of 0.005–3.0 V (vs. Li/Li^+) at a current densities of 200 mA g^{-1}. The charge–discharge capacities decrease during the first few cycles due to formation of stable electrolyte film formation as observed by other research groups.[1,2,20,21] The cycling data suggests that the nanostructured CeO_2 electrode is highly stable and reversible during repeated lithium insertion and extraction kinetics. The Coulombic efficiency after 10th cycles was more than 98%. Figure 4 shows the rate performance of CeO_2 hollow nanosphere anode at different current densities. The charge–

discharge capacities decrease with increase of current densities similar to other transition metal oxide-based nanostructured electrodes. The CeO_2 anode delivers discharge capacities of 639, 452, 280, and 188 mA h g^{-1} during the first cycle at current densities of 100, 400, 1000, and 2000 mA g^{-1}, respectively. More importantly, the electrode regains its high discharge capacity when the current density is lowered again to 200 mA g^{-1}. In addition, we have also performed the electrochemical performance of dense CeO_2 particles (Figures S3 and S4, Supporting Information).[22] As seen from Figure S3, the dense particles deliver a capacity of merely 60 mA h g^{-1} after 50 repeated cycles with 32.4% of Coulombic efficiency in the first cycle. The enhanced cycling performance and capacity retention of anode based on CeO_2 hollow nanospheres is attributed to the nanosize effect with a thin shell of about 5.5 nm. The nanosized shell-domain of hollow particles highly favors fast lithium intercalation–deintercalation during consecutive charge–discharge cycling. In addition, the hollow void space could also serve as effective buffering medium to prevent volume change and mechanical failure of electrodes.

In conclusion, we have demonstrated the fabrication of CeO_2 hollow nanospheres with average particle size of 28 ± 2 nm, and the particles are highly crystalline with face-centered cubic lattice structure. The hollow particle-based electrode delivered a capacity of 291 mA h g^{-1} after 100 cycles of charge–discharges. The CeO_2-constructed anode shows desirable electrochemical properties such as high capacity retention and good rate capability.

One of the authors (KN) thanks for a Grant-in-Aid for Scientific Research (No. 20310054) from the Japan Society for the Promotion of Science (JSPS).

References and Notes

1 J.-M. Tarascon, M. Armand, *Nature* **2001**, *414*, 359.
2 A. S. Aricò, P. Bruce, B. Scrosati, J.-M. Tarascon, W. van Schalkwijk, *Nat. Mater.* **2005**, *4*, 366.
3 M. S. Whittingham, *Chem. Rev.* **2004**, *104*, 4271.
4 X. W. Lou, L. A. Archer, Z. Yang, *Adv. Mater.* **2008**, *20*, 3987.
5 C. Sun, Z. Xie, C. Xia, H. Li, L. Chen, *Electrochem. Commun.* **2006**, *8*, 833.
6 H. Imagawa, A. Suda, K. Yamamura, S. Sun, *J. Phys. Chem. C* **2011**, *115*, 1740.
7 L. Li, H. K. Yang, B. K. Moon, Z. Fu, C. Guo, J. H. Jeong, S. S. Yi, K. Jang, H. S. Lee, *J. Phys. Chem. C* **2009**, *113*, 610.
8 C. Xu, R. Zeng, P. K. Shen, Z. Wei, *Electrochim. Acta* **2005**, *51*, 1031.
9 C. L. Campos, C. Roldán, M. Aponte, Y. Ishikawa, C. R. Cabrera, *J. Electoanal. Chem.* **2005**, *581*, 206.
10 S. McIntosh, J. M. Vohs, R. J. Gorte, *Electrochim. Acta* **2002**, *47*, 3815.
11 S. Park, R. Craciun, J. M. Vohs, R. J. Gorte, *J. Electrochem. Soc.* **1999**, *146*, 3603.
12 B. C. H. Steele, P. H. Middleton, R. A. Rudkin, *Solid State Ionics* **1990**, *40–41*, 388.
13 D. Liu, K. Nakashima, *Inorg. Chem.* **2009**, *48*, 3898.
14 S.-i. Yusa, Y. Yokoyama, Y. Morishima, *Macromolecules* **2009**, *42*, 376.
15 L. Mao, C. Liu, *Mater. Res. Bull.* **2008**, *43*, 1384.
16 W. Li, F. Cheng, Z. Tao, J. Chen, *J. Phys. Chem. B* **2006**, *110*, 119.
17 J. S. Chen, Y. L. Cheah, S. Madhavi, X. W. Lou, *J. Phys. Chem. C* **2010**, *114*, 8675.
18 C. Lu, L. Qi, J. Yang, X. Wang, D. Zhang, J. Xie, J. Ma, *Adv. Mater.* **2005**, *17*, 2562.
19 F. Zhou, X. Ni, Y. Zhang, H. Zheng, *J. Colloid Interface Sci.* **2007**, *307*, 135.
20 W. Xing, J. R. Dahn, *J. Electrochem. Soc.* **1997**, *144*, 1195.
21 S. R. Mukai, T. Hasegawa, M. Takagi, H. Tamon, *Carbon* **2004**, *42*, 837.
22 Supporting Information is available electronically on the CSJ-Journal Web site, http://www.csj.jp/journals/chem-lett/index.html.

